

Chapter 4

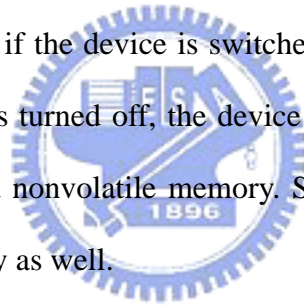
Experimental Results and Discussion of Electrical Properties

4.1 Electrical Properties

In order to focus on the measurement of electric properties and decrease factor of experiment, except the discussion of bistable sample, the all of the experiment sample is 0.04 M solution BTO. The most important part of a nonvolatile memory is the electrical properties. Including the switching voltage, operation voltage, retention time, and endurance are the properties trying to improve and focus on it. In addition, changing the different pre-process and post-process were tried. In the pre-process, the different mix method of BTO solution had been already tried. In the post-process, the different deposition temperature, thermal treatment temperature, thickness of thin film and different electrodes had been also tried. All the producing process will affect the electric properties and is going to be introduced and compared in the following. The voltage sweep is to use 4155C to sweep voltage and change the conductivity. In this section, what kind of experiment conditions can induce switching will be discussed. Including the preparation method of solution, thermal treatment temperature, and ambience, then the analysis of the leakage current, switch voltage, conductivity ratio in different experiment conditions, and the leakage of different state will be explained by different mechanisms. Besides, there are some other testing such as stress and retention.

4.2 Resistive Switching by Voltage Sweep

The I-V curve has sharp slopes when the applied voltage is swept to positive high voltage or negative high voltage, as Figure 4-1 shows. Before resistive switching is observed, a forming process is needed to initiate the BTO memory device by performing an electrical stress with a specific current compliance. In Figure 4-1, the typical resistive switching I-V characteristics of the Pt/BTO/LNO/Pt device are demonstrated, showing that both positive and negative voltage biases can switch the memory state from low resistance state (ON state) to high resistance state (OFF state), and via versa (Figure 4-3 the non-polar resistive switching). As those processes can be repeated at least is over 100 times, it means that the write-erase process of RRAM is repeatable. In addition, if the device is switched to high/low conductivity, and then the electric power supply is turned off, the device will stay at the same conductivity. This means that RRAM is a nonvolatile memory. So it is known that RRAM is repeatable and nonvolatile memory as well.



4.2.1 Different Leakage Current of Three States

Figure 4-1 shows the I-V curve of the Pt/BTO/LNO/Pt device which is fabricated at 400°C. Before any change, the resistance of the device is in the state of high resistance which is defined as original-state. When a negative voltage is applied, the leakage current density will increase with the applied voltage. At the voltage about -3.5V, the leakage current density increases sharply and jumps to the low resistance state which is defined as ON-state. The next, if the device is swept with an increasing negative voltage, the leakage current density will increase at the same time. At the voltage about -1V, the leakage current density decreases sharply and jumps to the high resistance state which is

defined as OFF-state. The most interesting part is the leakage current density of OFF-state is higher than its original-state. While sweeping the voltage to about -3.5V, the leakage current density will sweep to ON-state again. However, the typical resistive switching I-V characteristics of the Pt/BTO/LNO/Pt device are demonstrated, showing that both positive and negative voltage biases can switch the memory state from low resistance state (ON state) to high resistance state (OFF state), and via versa. (i.e. the non-polar resistive switching).

4.2.2 Electrical Properties of Forming Phenomenon

At first, we characterize the electrical properties in steady state. Current-Voltage (I-V) characteristics of this device are shown in Figure 4-1. The device was at OFF -state (low leakage current) as it was initially fabricated. When we sweep the applied voltage to a negative value of about -5V (Figure 4-3), the leakage current suddenly increases and switches to the ON-state. Subsequently, we make switching different device to 40 times, and statistics to forming voltage distributions as show in figure 4-4. In our experiment, platinum (Pt) is used to be top electrode, and LNO/Pt is used to be bottom electrode. As G. DEARNALEY claimed, "I-V curve development called forming process as the amplitude of the applied sinusoidal voltage is increased through the forming voltage." The minimum applied voltage which begins to induce conductivity changing is defined as forming voltage [11]. Forming phenomenon also exists in our samples. When applied voltage reaches to forming voltage, the conductivity changing character happens, as showed in figure 4-5. G. DEARNALEY also suggested that forming behavior in insulator was activated by one of thermally activated mechanism, giving a current I , where

$$\ln(I) \propto (V^{1/2})$$

In illustration of figure 4-5, the curve fitting of thermally activated mechanism. Formed leakage current of our sample that shows highly linear relation confirms the statement of G. DEARNALEY. In conclusion, the forming process, which should be a key point for conductivity switching phenomenon, could help us to understand the conductivity mechanism of our sample.

4.2.3 Bistable Sample

The sample of RRAM can be switched to different resistance states by sweep voltage. In this experiment, platinum was deposited on thin film as top electrode and LNO/Pt as bottom electrode contact node. The Current-Voltage (I-V) characteristics of this device are shown in Figure 4-1. The pyrolysis temperature is 400°C /30 minutes will have the bistable phenomenon. From the illustration it is known that the device is at very low conductivity at its initial state. Figure 4-6(a) shows the negative voltage which is applied on the device and swept to about -3.5V, the leakage current increases and switches immediately to the ON-state (low resistance state), but the voltage sweep back to -1V, the leakage current decreases and switches back to OFF-state.

Figure 4-6(b) when the negative voltage which is applied on the device and swept to about -3.5V, the leakage current increases and switches immediately to the ON-state, but the voltage sweep to 1.2V, the leakage current decreases and switches back to OFF-state. Figure 4-6(c) shows the positive voltage which is applied on the device and swept to about 4V, the leakage current increases and switches immediately to the ON-state, but the voltage sweep to 1.2V, the leakage current decreases and switches back to OFF-state. Figure 4-6(d) when the positive voltage which is applied on the

device and swept to about 4V, the leakage current increases and switches immediately to the ON-state, but the voltage sweep to -1V, the leakage current decreases and switches back to OFF-state. From the illustration, it can also be owned that the switching voltage of ON-state and OFF-state are symmetric. The voltage of switching OFF-state to ON-state is higher than switching from ON-state to OFF-state. From the illustration Figure 4-1, it is found that the ratio of ON-state is over OFF -state about 10000 times (Figure 4-2). The resistive switching behavior is reproducible and can be traced over 100 times. The resistance and operation voltage distributions of both ON and OFF state among 100th cycles in a single Pt/BTO/LNO/Pt device are shown in Figure4-7(a) and (b). The resistance distributions of switching 40 devices are investigated as shown in Figure4-8(a) and (b). The variations within the resistance distributions might be due to the uniformity of the BTO thin film fabricated by sol-gel method, but the resistance ratio between R_{on} and R_{off} is still over 100 times (Figure4-9). Therefore, the variations present in R_{on} , R_{off} , V_{on} , and V_{off} of the Pt/BTO/LNO/Pt device, which might be due to the random formation and rupture of the conducting filaments. In spite of the variations of R_{on} and R_{off} , the resistance ratio between R_{on} and R_{off} at least is over 1000 times.

4.3 Thermal Treatment Effect

In order to change the electrical properties, the BTO thin film was in the thermal treatment process. Figure 4-10 indicates the leakage current density vs. bias voltage illustration. From the illustration, it shows that the OFF-state leakage current density will increase with the thermal treatment temperature. From the XRD analysis Figure 3-3, it is easy to find when the thermal treatment temperature higher than 500⁰C , the BTO

thin film will have the phase change phenomenon. The higher thermal treatment temperature, the higher degree of crystallization of BTO thin film, this could be the reason of OFF-state leakage current density with increasing thermal treatment temperature. The OFF-state leakage current will increase with increasing thermal treatment temperature increasing, but the ON-state leakage current won't change too much. This phenomenon leads to conclude that the current ratio will decay with increasing thermal treatment temperature.

4.4 Retention Test

It is very important for a nonvolatile memory device its memory state to keep long time its memory. The data storage time, called retention time, is a significant landmark. It means that how long the resistance values are kept in the two states. As showed in Figure 4-11, the retention time of the two states is at least over 10^6 seconds and the resistance ratio still keeps over 10000 times, which does not be affected by the operation of the memory readout. But it is also very difficult to measure a memory device at room temperature for a very long time. In order to avoid the tedious retention testing, the thermal acceleration was used to test the memory retention state. We also test the retention under the 85°C as show in Figure 4-12, obviously, the leakage current density of the OFF-state has a little decay. After the thermal acceleration testing, the OFF-state leakage current density decreased a lot.

Although the leakage current density of OFF-state was decreased, the retention time under the high temperature is at least over 106 seconds, too. And the windows ratio still keeps over 100 times. It means that it will not induce any problem as being a memory device in the readout process.

4.5 Stress Test

To go a step further to confirm the reliability of data storage in higher bias voltage, a stress testing had been done. Fig. 4-13 shows the leakage current density of ON-state and OFF-state versus the stress time. After more than three hours with applying 0.3V voltage on the device, it is clearly shown that the leakage current of different states are maintained at the same leakage order. It means that the voltage stress will not disturb the memory state. Therefore, the device has the non-destructive readout property. After large current density stresses, the leakage current densities of the device for different states do not increase, indicating that the device has the excellent electrical and memory properties. Beside of room temperature, we also test the stress under the high temperature 85°C in order to accumulate the time effect, as show in Fig.4-14. The ON-state is stable as room temperature. The OFF-state conductivity is higher but the resistive ratios still keep over 4 orders. In other words, the device still shows good performers under the high temperature stress test.

4.6 Endurance Test

In spite of different I-V curve of Pt/BTO/LNO/Pt device, the resistive switching could be reproduced and successively switching the device to OFF-state and then back to ON-state by the dc voltage sweep method was observed. The 10th, 50th, 100th, I-V curve of Pt/BTO/LNO/Pt device are shown in Fig. 4-15, and there is a little distortion between them. During the successive resistive switching by dc voltage method, there is no “set fail” phenomenon observed. The “set fail” phenomenon is a failure of resistive switching from OFF-state to ON-state. Moreover, as the continuous resistive switching cycle increases, the OFF-state current gradually increase, which causes the resistance

ratio between ON-state and OFF-state to decrease.

4.7 Fitting Leakage Current

From the Physics of Semiconductor Devices [31], there are six different basic conduction processes in semiconductors: Schottky emission, Frenkel-Poole emission, tunneling or field emission, space-charge-limited, Ohmic, and Ionic conduction. In order to find the mechanism of three different states, high-state, low-state, and original-state, the I-V curves of three different states have been re-calculated to fit the mechanism. The I-V characteristics are indicated in Figure 4-16, which is obtained from typical I-V curve within $\pm 2V$, in a double natural logarithm plot. Due to the slope of the ON -state and OFF-state in low electrical field region is very close to 1, the conduction mechanisms under low electrical field ($-4.6 \sim -2 V$) is believed to be satisfied with Ohmic conduction. At higher voltage bias, the conduction mechanism of ON-state still obeys Ohmic conduction, implying that Ohmic conduction dominates the carrier transport in ON-state but it is not suitable for OFF-state. Figure 4-17 depicts the conduction mechanism of OFF-state in both positive and negative regions under electrical field voltage region from $-2 V$ to $0.5 V$ is space charge limit current (SCLC)

by curve fitting. The space charge limit current equation is $J = \frac{8\epsilon\mu V^2}{9d^3}$. Furthermore, the carrier conduction in high electrical field voltage region from $0.5 V$ to $2 V$ (Figure 4-18) is dominated by Frenkel-Poole emission mechanism as shown in the of Figure 4-19(a)

and (b). Equation is $J \sim V \exp\left(\frac{+2a\sqrt{V}}{T} - \frac{q\Phi_B}{kT}\right)$.

Therefore, the conduction mechanisms dominating in the ON-state is Ohmic conduction and OFF-state is Ohmic conduction, space charge limit current, and Frenkel-Poole emission. From Figure 4-16 and Figure 4-17 show the natural logarithm

plots of the I-V curve for the positive and negative-voltage regions. The I-V characteristics exhibiting the $I \propto V$ correlation is Ohmic (slope = 1), and followed by $I \propto V^2$ correlation SCLC (slope = 2). From the I-V curve that has been shown, the leakage current density of the OFF/ON state shows high symmetry at both positive and negative voltage. As the same reason, the mechanism of the device was conjectured due to the bulk but not interface.



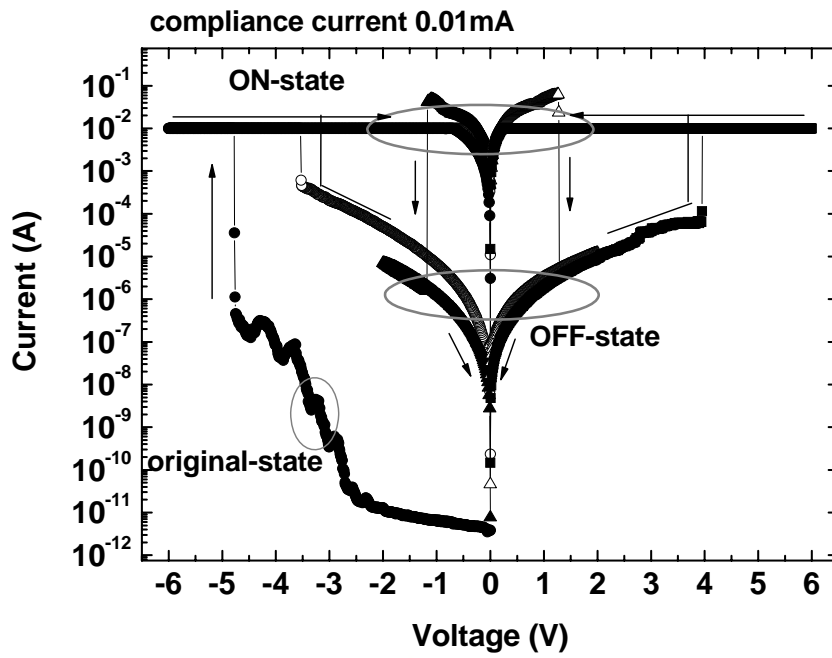


Fig. 4-1 Typical resistive switching I-V curve of Pt/BTO/LNO/Pt device

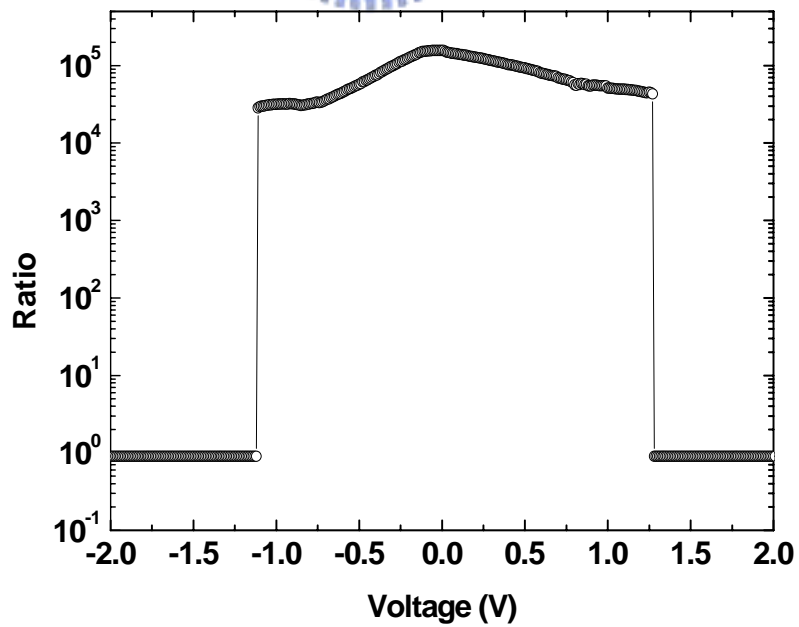


Fig.4-2 Resistance ratio of Pt/BTO/LNO/Pt device

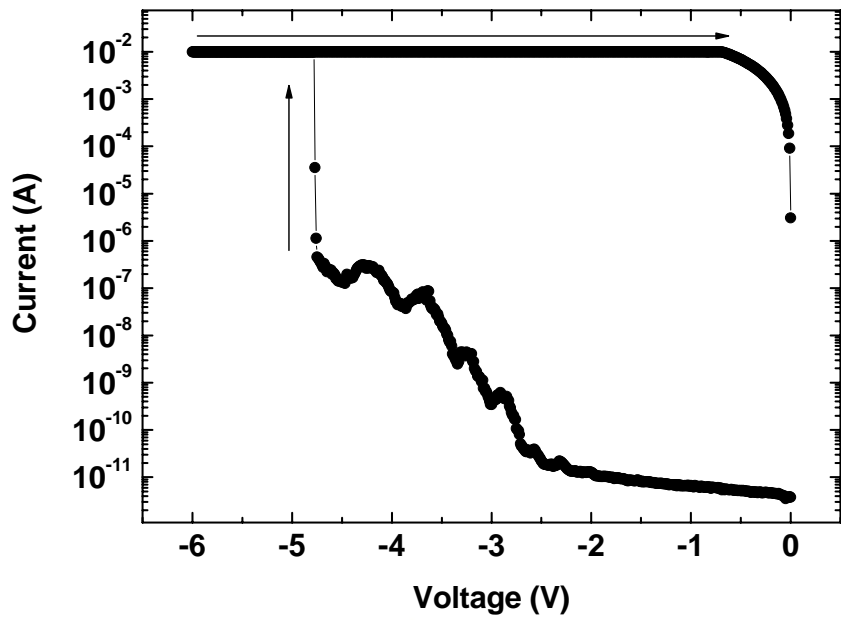


Fig. 4-3 I-V curve of forming phenomenon

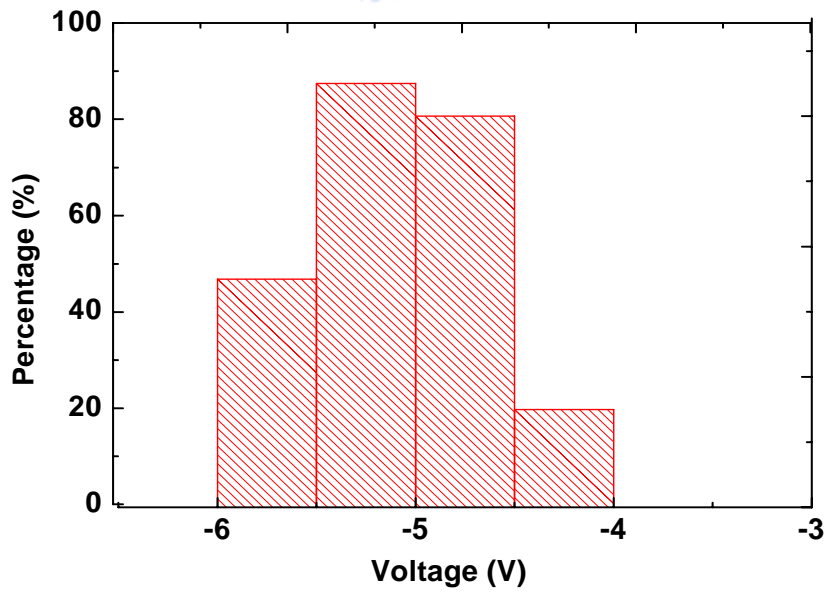


Fig. 4-4 Forming voltage distributions among 40 devcies

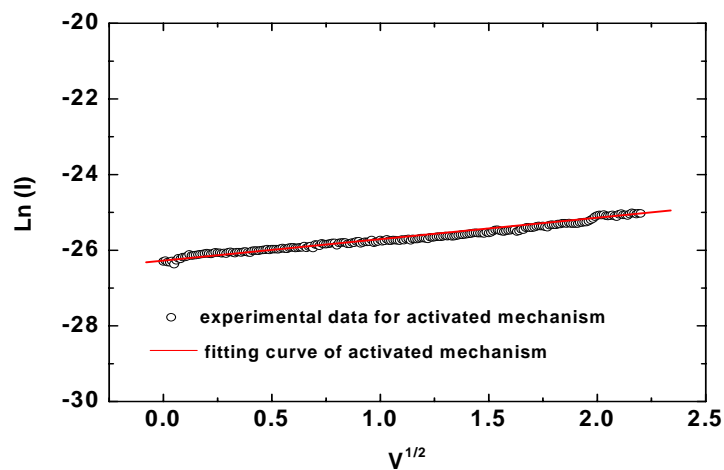


Fig. 4-5 Thermally activated mechanism fitting of forming leakage

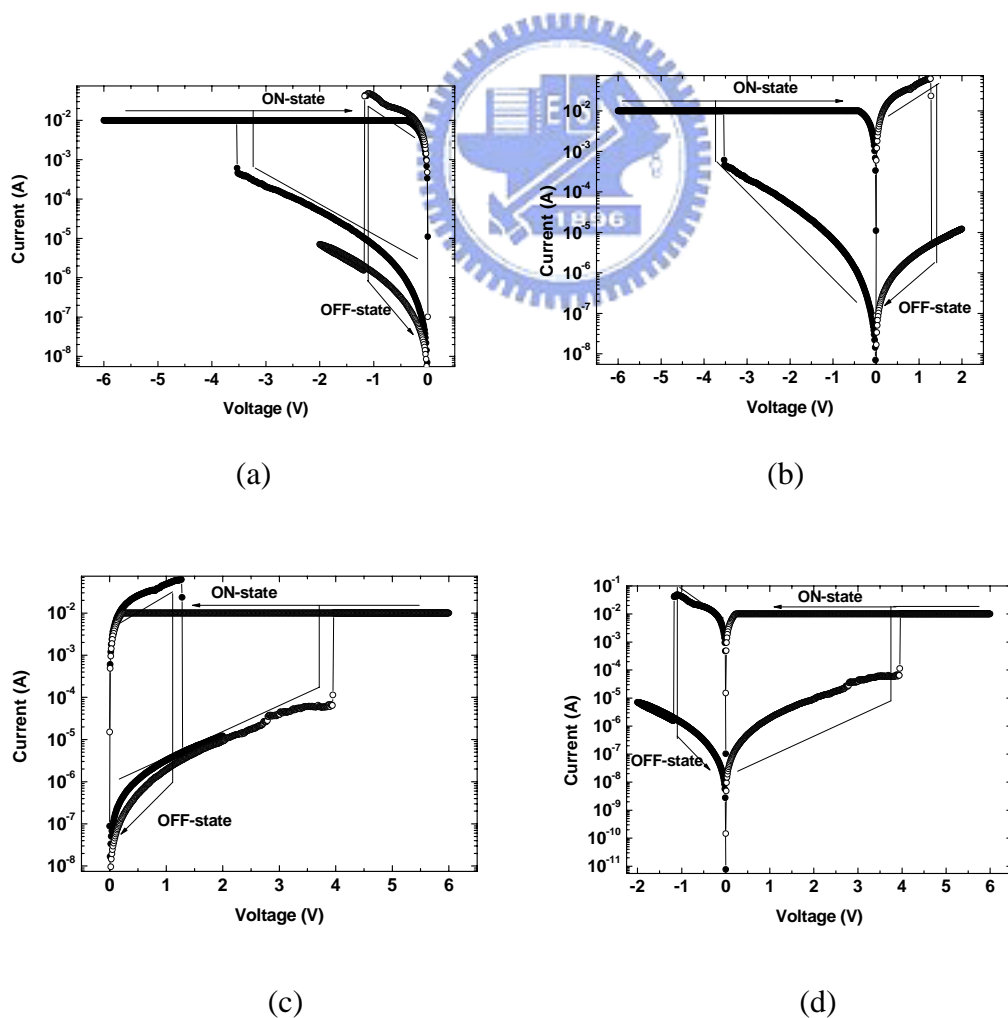
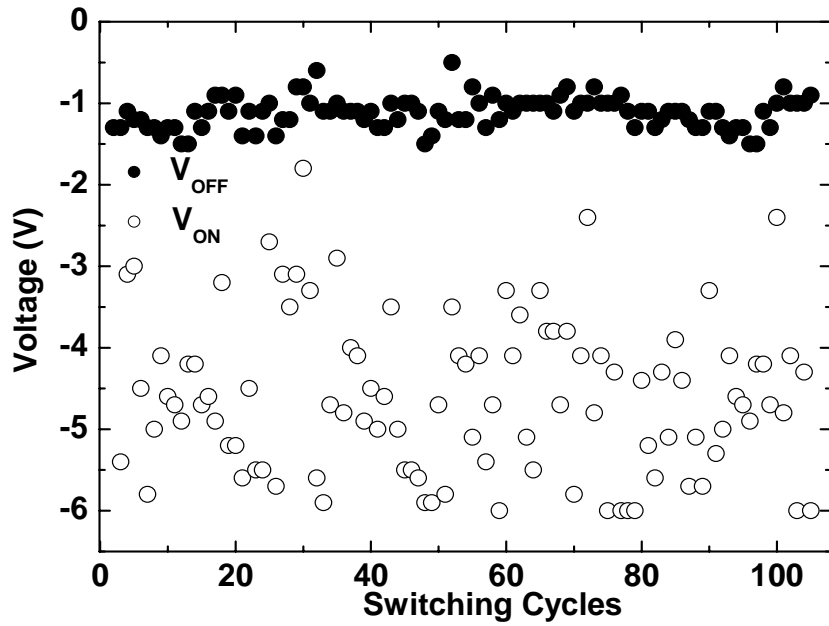
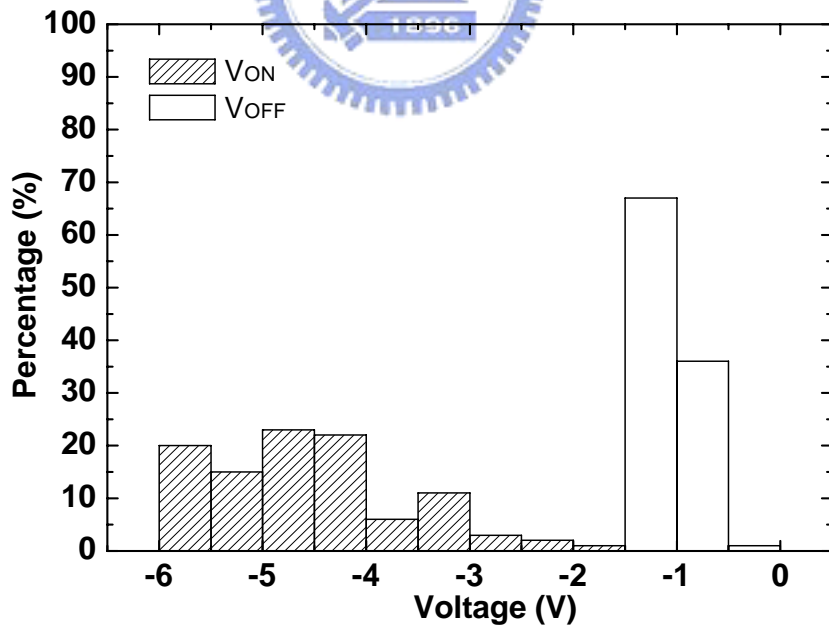


Fig. 4-6 The non-polar resistive switching

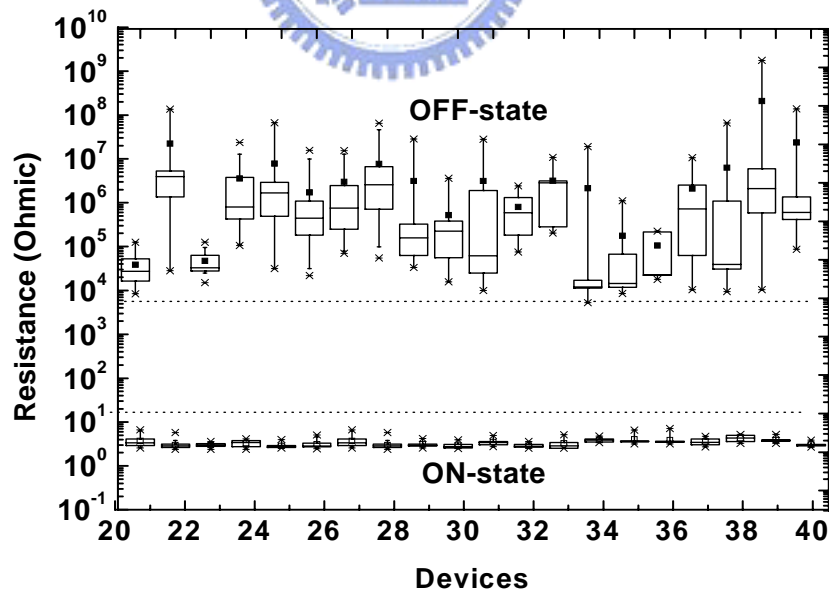
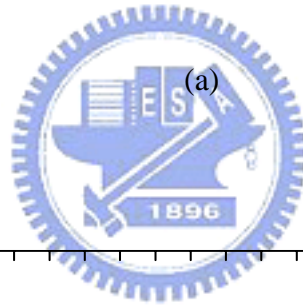
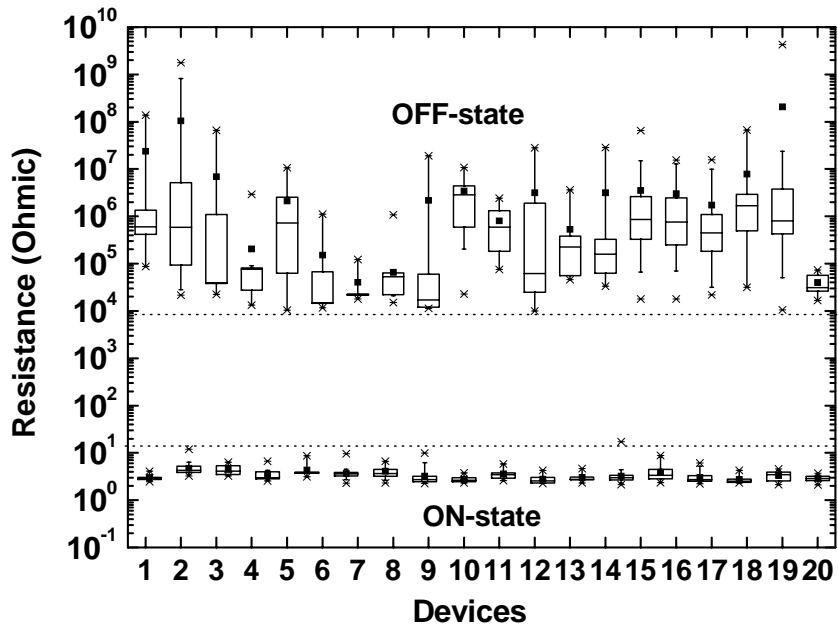


(a) Over 100 write/erase cycles test for ON-state and OFF-state



(b) Operation voltage statistical graph among 100 cycles

Fig. 4-7 Operation voltage distributions among 100th cycles in a single Pt/BTO/LNO/Pt device



(b)

Fig. 4-8 Statistical resistance distributions of switching 40 devices

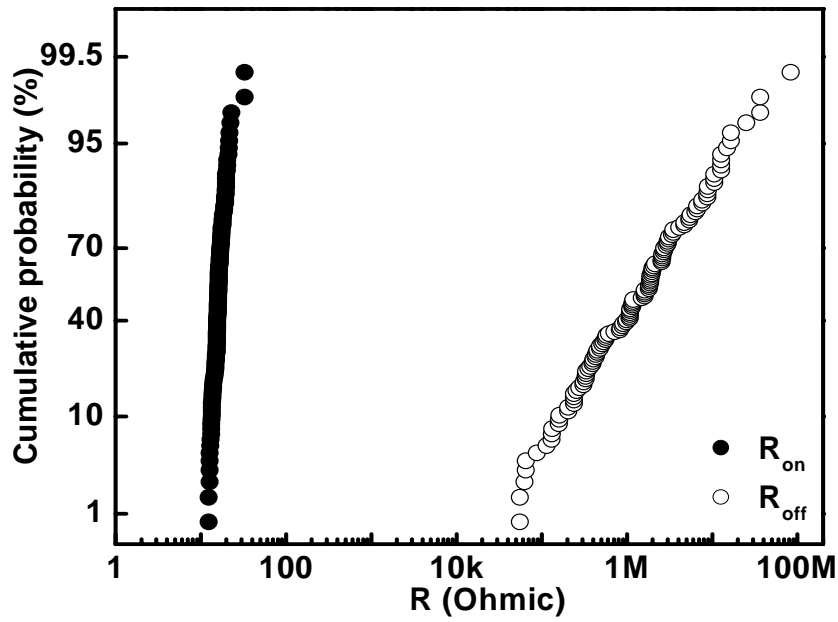


Fig. 4-9 Resistance distributions of both ON and OFF states among 100 cycles in a single Pt/BTO/LNO/Pt device

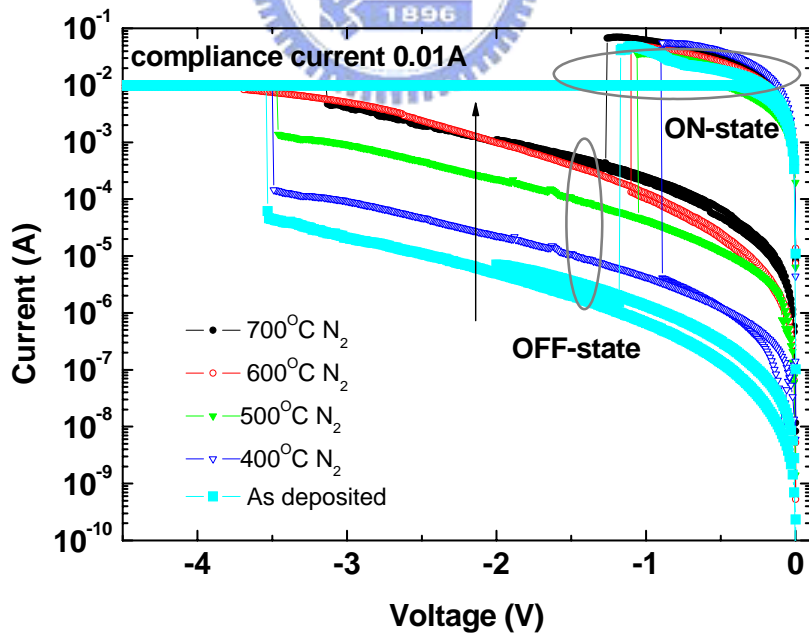


Fig. 4-10 Low-state of thermal treatment at various temperatures

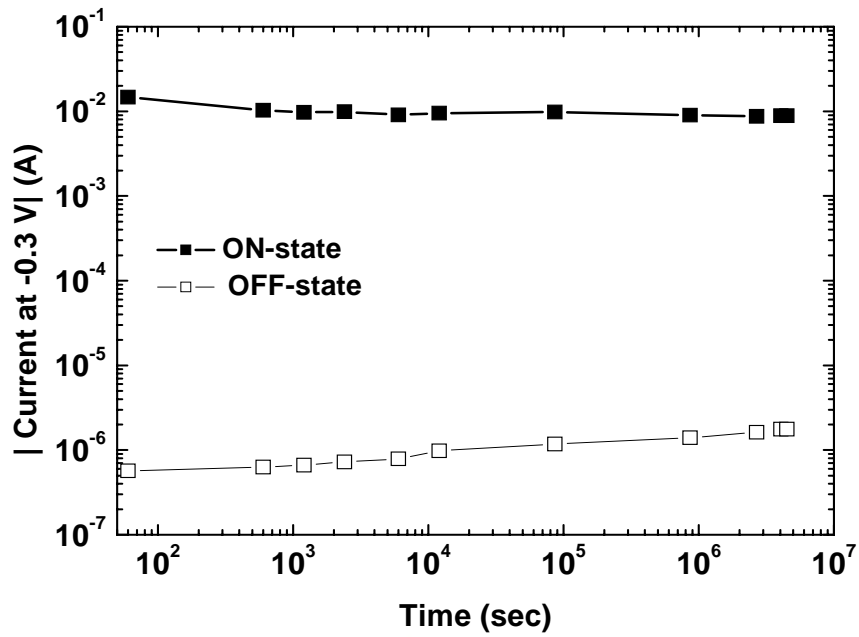


Fig. 4-11 ON-state and OFF-state retention at RT

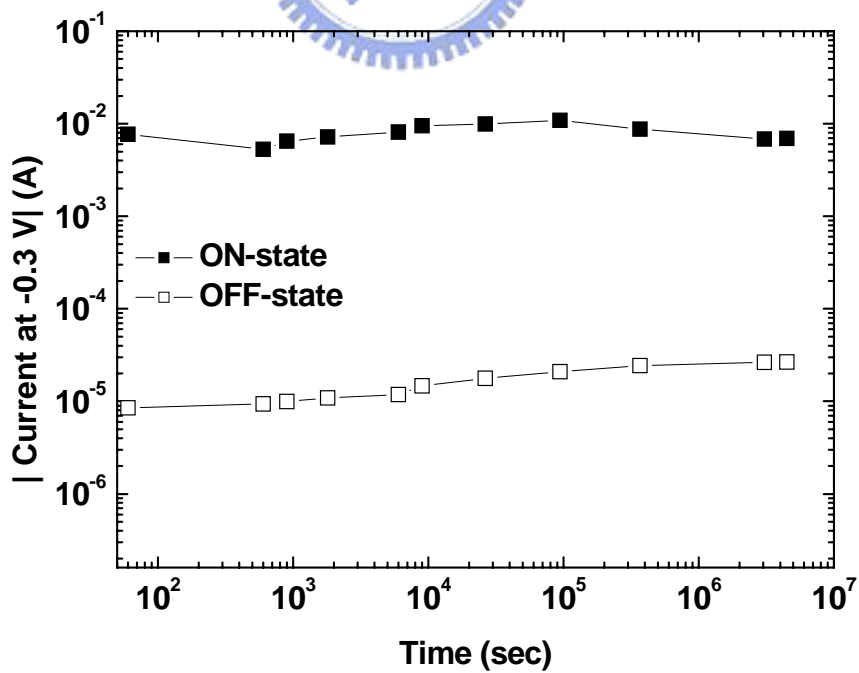


Fig. 4-12 ON-state and OFF-state retention at 85°C

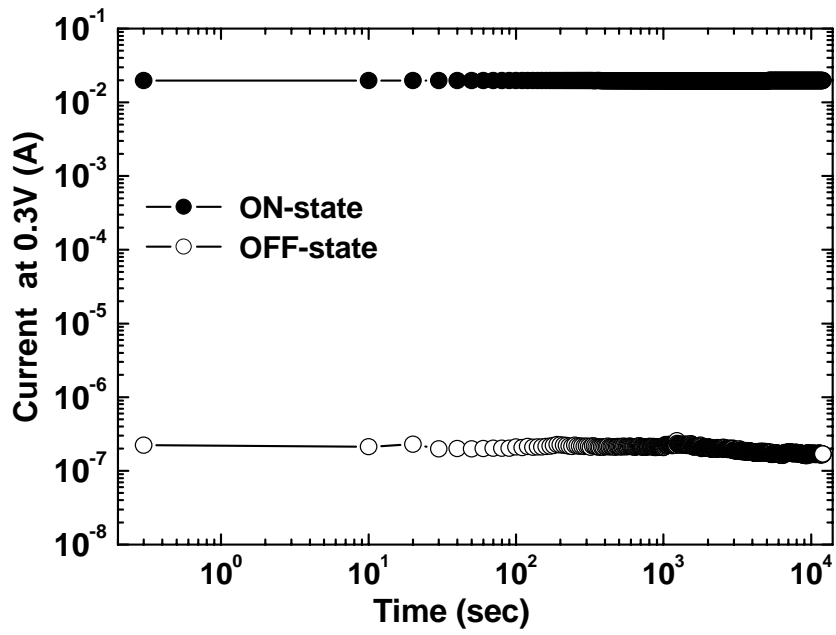


Fig. 4-13 ON-state and OFF-state Stress at RT

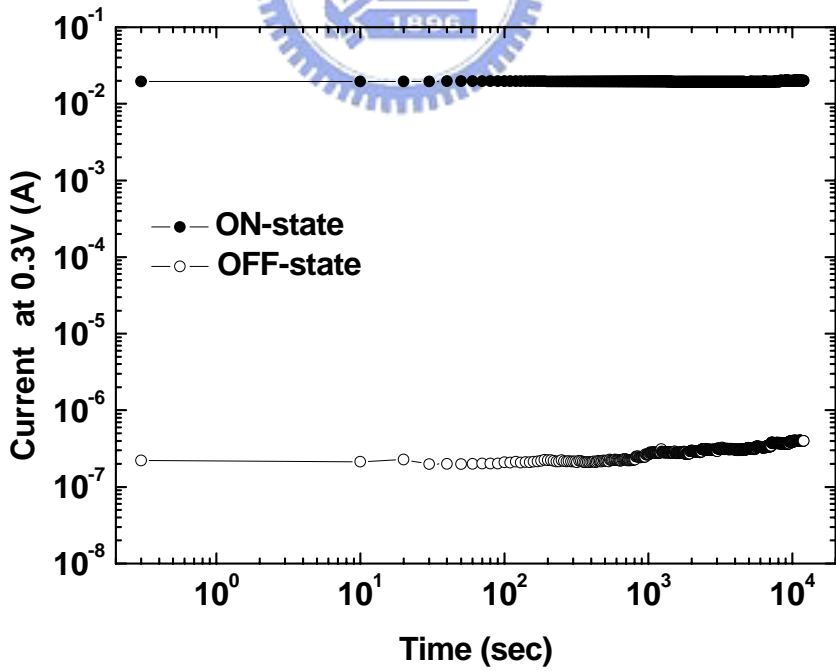


Fig. 4-14 ON-state and OFF-state at 85⁰C

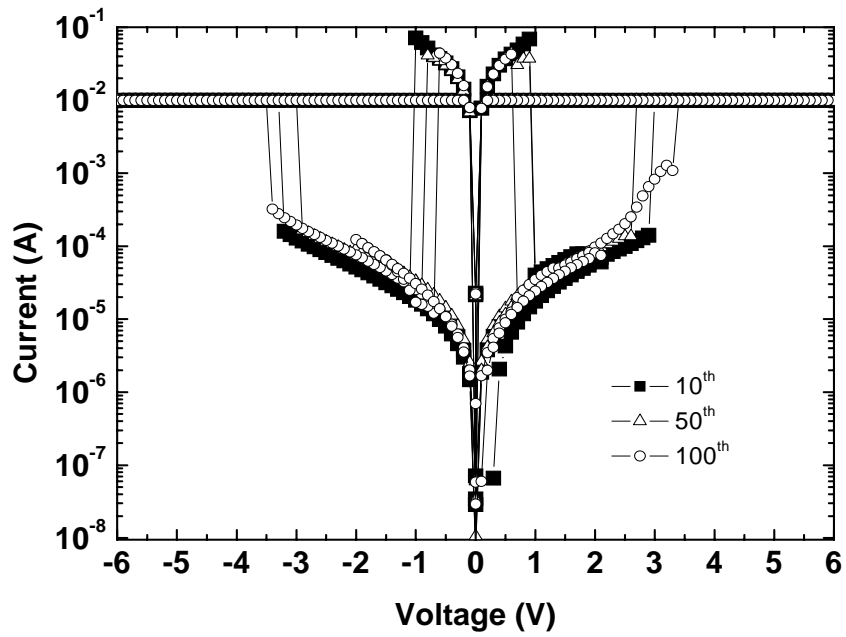


Fig. 4-15 10th, 50th, 100th I-V curves during continuous dc voltage resistive switching cycles

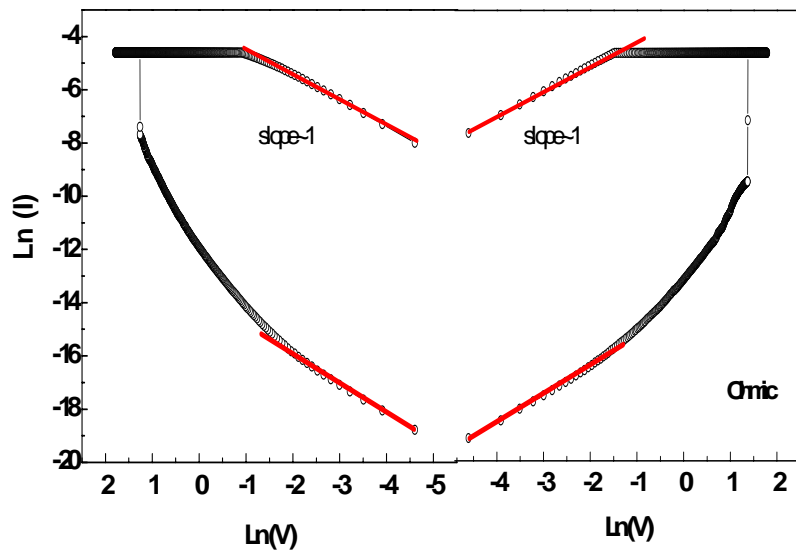
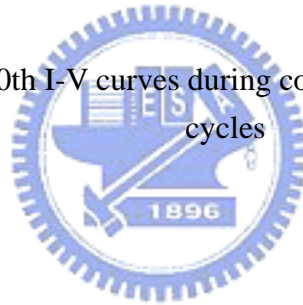


Fig. 4-16 I-V curve fitting in low electrical field

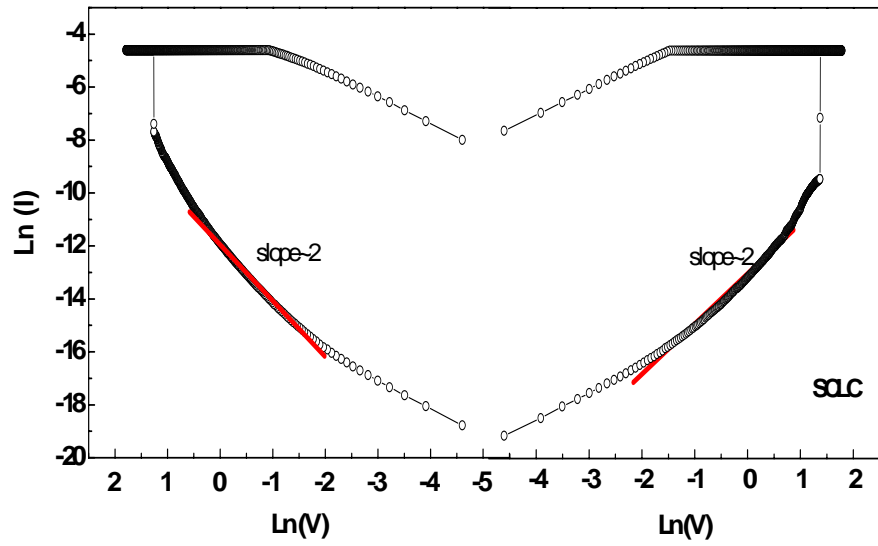


Fig. 4-17 I-V curve fitting in middle electrical field

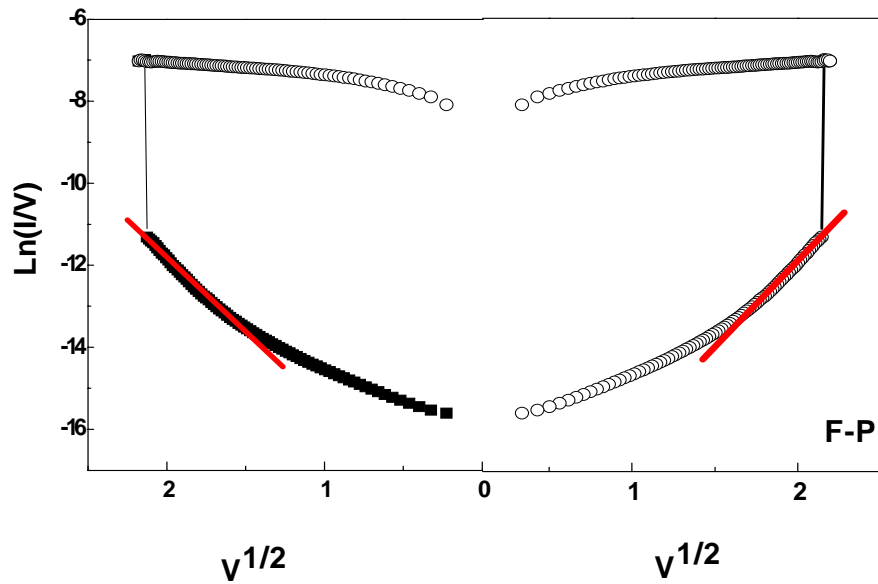
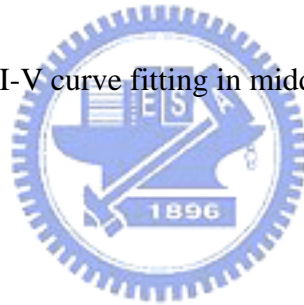
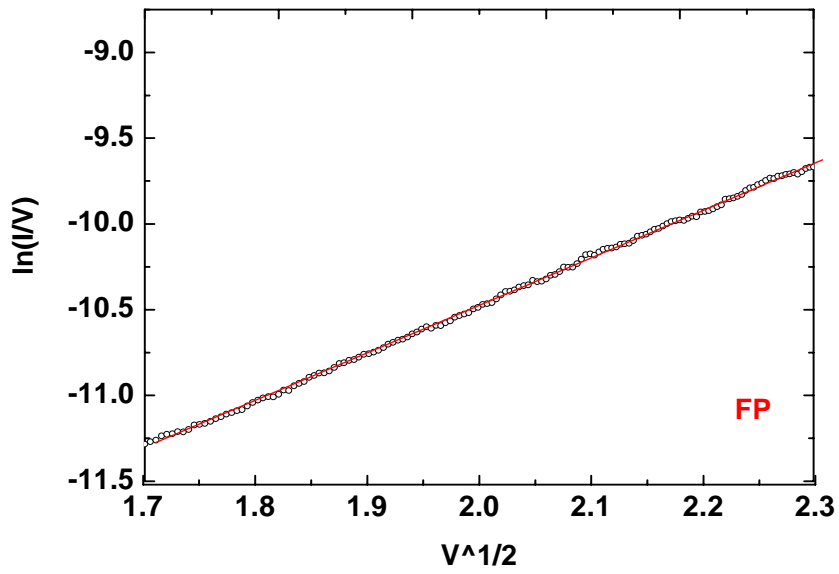


Fig. 4-18 I-V curve fitting in high electrical field

(a)



(b)

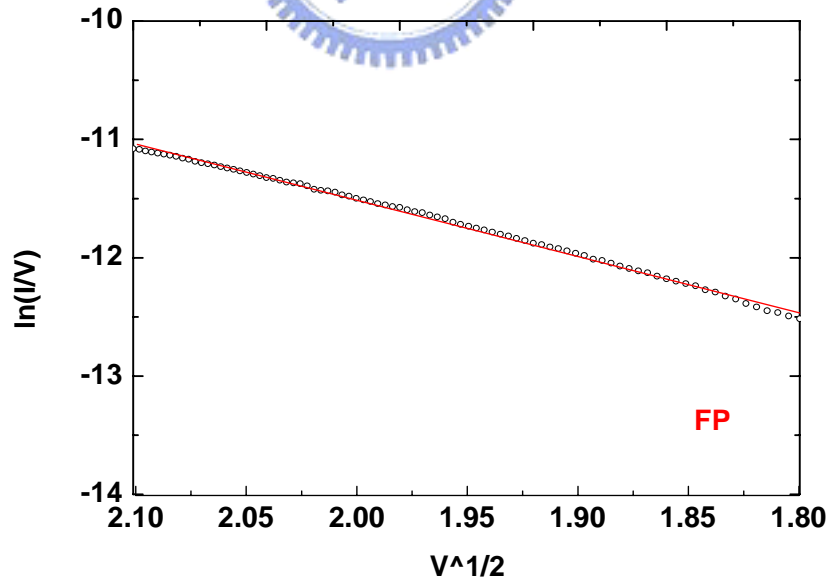


Fig. 4-19 I-V curve fitting in high electrical field (a) fitting in positive region (b) I-V curve fitting in negative region